npg

Original Article

Gene expression profiles of human liver cells mediated by hepatitis B virus X protein

Wei-ying ZHANG[1], Fu-qing XU[1], Chang-liang SHAN[1], Rong XIANG[3], Li-hong YE[2,*], Xiao-dong ZHANG[1,*]

[1]Department of Cancer Research, Key Laboratory of Molecular Microbiology and Technology of Ministry of Education, Institute for Molecular Biology, College of Life Sciences; [2]Department of Biochemistry, College of Life Sciences, [3]School of Medicine, Nankai University, Tianjin 300071, China

Aim: To demonstrate the gene expression profiles mediated by hepatitis B virus X protein (HBx), we characterized the molecular features of pathogenesis associated with HBx in a human liver cell model.
Methods: We examined gene expression profiles in L-O2-X cells, an engineered L-O2 cell line that constitutively expresses HBx, relative to L-O2 cells using an Agilent 22 K human 70-mer oligonucleotide microarray representing more than 21,329 unique, well-characterized Homo sapiens genes. Western blot analysis and RNA interference (RNAi) targeting HBx mRNA validated the overexpression of proliferating cell nuclear antigen (PCNA) and Bcl-2 in L-O2-X cells. Meanwhile, the BrdU incorporation assay was used to test cell proliferation mediated by upregulated cyclooxygenase-2 (COX-2).
Results: The microarray showed that the expression levels of 152 genes were remarkably altered; 82 of the genes were upregulated and 70 genes were downregulated in L-O2-X cells. The altered genes were associated with signal transduction pathways, cell cycle, metastasis, transcriptional regulation, immune response, metabolism, and other processes. PCNA and Bcl-2 were upregulated in L-O2-X cells. Furthermore, we found that COX-2 upregulation in L-O2-X cells enhanced proliferation using the BrdU incorporation assay, whereas indomethacin (an inhibitor of COX-2) abolished the promotion.
Conclusion: Our findings provide new evidence that HBx is able to regulate many genes that may be involved in the carcinogenesis. These regulated genes mediated by HBx may serve as molecular targets for the prevention and treatment of hepatocellular carcinoma.

Introduction

Hepatitis B virus (HBV) infection is one of the major risk factors for the development of hepatocellular carcinoma (HCC)[1]. However, the mechanism of HBV-induced HCC remains unclear[2]. The HBV genome is a partially double-stranded DNA molecule with four open reading frames (ORFs) termed S, C, P, and X[3]. The X gene of HBV (HBx) encodes a 154 amino acid polypeptide that is essential for viral infection and replication and plays a crucial role in the development of HCC[4]. Although HBx does not bind to DNA, it exerts a pleiotropic effect on diverse cellular functions as a transcriptional co-activator. HBx exhibits many activities *in vitro*. In a cell culture system, HBx is able to activate the transcription of host genes, such as c-Myc, as well as viral genes[5,6]. HBx is also involved in different cytoplasmic signaling pathways. The majority of HBx is localized in the cytoplasm, where it interacts with and stimulates protein kinases such as protein kinase C, Janus kinase/STAT, IKK, PI-3-K, stress-activated protein kinase/Jun N-terminal kinase, and protein kinase B/Akt. HBx induces centrosome hyperamplification and mitotic aberration by activation of the Ras-MEK-MAPK pathway, which may contribute to genomic instability during hepatocarcinogenesis[7]. HBx can transactivate various cellular transcriptional elements, such as AP-1, AP-2, NF-κB, and cAMP response element (CRE) sites. Consequently, HBx can affect the activities of various transcriptional elements in the host cell and elicit different cellular responses. Previously, we demonstrated that HBx upregulated both the expression and the activity of hTERT in hepatoma[8]. We also found that HBx was able to upregulate the expression of survivin, which suggests that survivin may be involved in the carcinogenesis of HCC that is mediated by HBx[9]. cDNA microarray is a powerful tool

* Correspondence to Prof Xiao-dong ZHANG and Prof Li-hong YE.
E-mail zhangxd@nankai.edu.cn (Xiao-dong ZHANG); yelihong@nankai.edu.cn (Li-hong YE)

for identifying disease-related gene expression profiles in biological samples. Using cDNA microarray, we examined gene expression profiles in a model of hepatoma cells stably transfected with HBx[10]. These data from the hepatoma cell model showed progressive changes during tumor development. However, the mechanism of hepatoma mediated by HBx remains unclear.

In the present study, we examined the gene expression profiles of L-O2-X cells by cDNA microarray analysis. When compared with the gene expression profiles of H7402-X cells[10], our findings provide new insight into the molecular mechanism of carcinogenesis mediated by HBx in human liver cells.

Materials and methods

Cell culture The human liver L-O2 cell line (purchased from Nanjing KeyGen Biotech Co Ltd, Nanjing, China), which originated histologically from normal human liver tissue that had been immortalized by stable transfection of the hTERT gene, was used previously[9, 11–13]. L-O2-P (cell line from L-O2 cells stably transfected with empty pcDNA3 plasmid) and L-O2-X (cell line from L-O2 cells stably transfected with the HBx gene) were established as described previously[13]. L-O2, L-O2-P, and L-O2-X cells were cultured in RPMI-1640 medium (GIBCO, USA) containing 100 U/mL penicillin, 100 µg/mL streptomycin and 10% fetal calf serum. Cultures were incubated in a humidified atmosphere with 5% CO_2 at 37 °C.

Gene expression profiling analysis An Agilent 22 K human 70-mer oligonucleotide microarray (CapitalBio Corp, China) containing more than 21 329 unique, well-characterized Homo sapiens genes was used. Double-stranded cDNAs (containing the T7 RNA polymerase promoter sequence) were synthesized from 1 µg of total RNA using the CbcScript reverse transcriptase with cDNA synthesis system according to the manufacturer's protocol (CapitalBio Corp, China) with the T7 Oligo (dT). cDNA labeled with a fluorescent dye (Cy5 or Cy3-dCTP) was produced by Eberwine's linear RNA amplification method and the subsequent enzymatic reaction and was improved by CapitalBio. The Klenow enzyme labeling strategy was adopted after reverse transcription using CbcScript II reverse transcriptase. All procedures for hybridization and slide and image processing were carried out according to the manufacturer's instructions. The slides were washed, dried, and scanned using a confocal LuxScan™ scanner and the obtained images were then analyzed using LuxScan™ 3.0 software (both from CapitalBio Corp, China). The procedures were repeated for a replicate experiment with

independent hybridization and processing. For individual channel data extraction, faint spots for which the intensities were below 400 units after background subtraction in both channels (Cy3 and Cy5) were removed. A space- and intensity-dependent normalization based on a LOWESS program was employed. To avoid false positive results, multiple testing corrections were considered. In each experiment, three types of positive controls (Hex, four housekeeping genes, and eight yeast genes) and two types of negative controls (50% DMSO and twelve negative control sequences from the Operon Oligo database) were used. Each probe was printed in triplicate. Furthermore, we performed the fluorescence-exchange microarray analysis. We performed three independent cDNA microarray experiments to obtain more precise data. For two-color designs, intensity reproducibility was calculated both within and across the two different dyes to assess the impact of the dye on the resulting measurement. For within-dye calculations, the technical replicates of samples labeled with the same dye across the microarrays were considered, and for across-dyes calculations, all replicates for a given sample labeled with either dye were evaluated. Comparisons between the combinations of *P* values and fold-change thresholds were given, with the differentially expressed genes identified using a one-sample *t*-test of the sample B to sample A (B/A) ratio data, including five replicates for each site. Two *P* values ($P<0.05$ and $P<0.01$) and three fold-change (FC) thresholds (FC>1.5, FC>2.0 and FC>4.0) were acceptable in the microarray analysis.

RNA interference The HBV X gene was cloned into pSilencer 3.0 to create pSilencer 3.0-X. The following primers were used: sense, 5′-GATCCCGGTCTTACA-TAAGAGGACTTTCAAGAGAAGTCCTCTTATGT-AAGACCTTTTTTGGAAA-3′; antisense, 5′-AGCTTTT-CCAAAAAAGGTCTTACATAA GAGGACTTCTCTT-GAAAGTCCTCCTTATGTAAGACCGGG-3′[9]. The purified vector was transfected using Lipofectamine into L-O2-X cells for 36 h, as described previously[9]. The expression level of the HBx protein in L-O2-X cells was examined by Western blot analysis.

Treatment with an inhibitor of COX-2 According to the data, we found that the PTGS2 gene was upregulated in L-O2-X cells (Table 1). The PTGS2 gene encodes COX-2[14]. Therefore, we investigated the effect of HBx on COX-2 using an inhibitor of COX-2. The L-O2, L-O2-P, and L-O2-X cells were cultured as described above in a 6-well plate for 24 h, and then the cells were re-cultured in serum free medium for 12 h. Briefly, L-O2-X cells were treated with 50 µmol/L indomethacin (indo, Sigma-Aldrich, USA, inhibitor of COX-2) for 2 h. The level of COX-2 in the treated

L-O2 cells was examined by Western blot analysis. Meanwhile, the proliferation of L-O2-X cells treated with indo was examined by the BrdU incorporation assay.

Western blot analysis L-O2-X, L-O2-P, and L-O2 cells were lysed in protein lysis buffer (62.5 mmol/L Tris-HCl, pH 6.8, 2% SDS, 5% 2-mercaptoethanol, 10% glycerol) and the protein concentration was determined using the 2-D Quant kit (Amersham Biosciences, Buckinghamshire, UK). Following electro-transfer onto polyvinylidene difluoride membranes, the membranes were blocked with 5% non-fat dry milk in 0.1% Triton X 100-TBS (TTBS) and incubated overnight at 4°C with specific primary antibodies. The following primary antibodies were used as described previously[9, 15]: PCNA (NeoMarkers, Fremont, CA, USA, 1:1000 dilution); Bcl-2 (NeoMarkers, Fremont, CA, USA, 1:500 dilution); HBx (obtained from the Fox Chase Institute for Cancer Research, Philadelphia, Pa, USA, 1:50 000 dilution); COX-2 (NeoMarkers, Fremont, CA, USA, 1:200 dilution); and β-actin (NeoMarkers, Fremont, CA, USA, 1:1000 dilution). Staining was performed with an HRP-linked secondary antibody (GE Healthcare Bio-Science, USA). The protein bands were visualized by an enhanced chemiluminescence (ECL) kit according to the manufacturer's specifications (GE Healthcare Bio-Sciences, USA).

BrdU incorporation assay DNA synthesis was measured using a 5′-bromodeoxyuridine (BrdU, Sigma, USA) incorporation assay. Briefly, L-O2, L-O2-P, and L-O2-X cells were seeded in 24-well plates for 12 h, and then the cells were serum starved in defined medium overnight. Additionally, L-O2, L-O2-P, and L-O2-X cells were treated with 50 μmol/L indo for 4 h. The BrdU incorporation assay was performed according to a previously published protocol[16]. The BrdU labeling index was assessed by point counting through a Nikon TE200 inverted microscope (Nikon, Tokyo, Japan) using a 40×objective lens. A total of 700–800 nuclei were counted in 6–8 representative fields. The labeling index was expressed as the number of positively-labeled nuclei/total number of nuclei. All groups (*n*=3 in each group) were performed.

Statistical analysis All experiments were repeated independently, at least three times. Values are given as means±SD. The analyzed data from two groups were compared using Student's *t* test. A *P*<0.05 was considered statistically significant.

Results

Differential expression profiles in L-O2-X cells Previously, we investigated progressive changes in hepatoma

cells stably transfected with HBx and found some differentially expressed genes[10]. However, those data only showed the distinctive gene pattern in the context of heptoma. To distinguish the differential expression of genes in normal human liver L-O2 cells and hepatoma cells mediated by HBx, we examined the differential expression profiles in L-O2-X cells by cDNA microarray analysis (Figure 1). The cDNA microarray showed that the expression levels of 152 genes were remarkably altered, 82 of those genes were upregulated and 70 genes were downregulated in the L-O2-X cells. The altered genes were associated with signal transduction pathways, cell cycle, metastasis, transcriptional regulation, immune response, metabolism, and other processes (Table 1). To avoid false positive results, each probe was printed in triplicate using a SmartArray™ microarrayer (CapitalBio Corp Beijing, China). The cDNA microarray
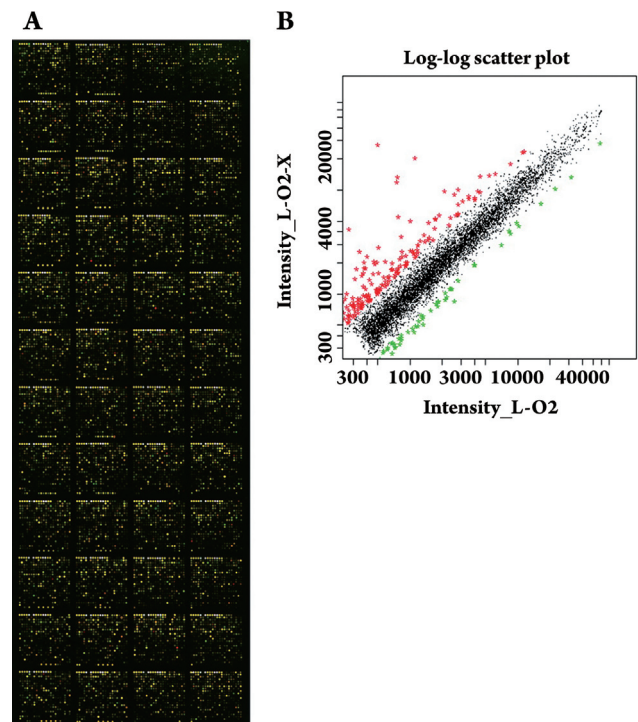

Figure 1. Examination of the L-O2-X gene expression profiles by cDNA microarray analysis. (A) A scanning image of the hybridizing signals on gene chips showed high expression (red), low expression (green), and no expression changes (yellow) between L-O2 and L-O2-X cells. (B) Scatter plot graph of Cy3-labeled and Cy5-labeled probes hybridizing with the microarray. Each point on the plot represented a gene hybridization signal. The black points represented ratios that ranged from 0.5 to 2.0 and belonged to the no difference group. The red points represented the ratios that were >2.0 and the green points represented the ratios that were <0.5, both of which indicate that gene expression was most probably altered.

Table 1. Gene expression profiles in L-O2-X cells compared with L-O2 cells by cDNA microarray. Each probe was printed in triplicate using a SmartArray™ microarrayer (CapitalBio Corp Beijing, China) in every slide. cDNA microarray was the fluorescence-exchange microarray. Three independent cDNA microarray analysis were performed.

Accession No	Abbreviation	Up- or down-regulation	Ratio1	Ratio2	Accession No	Abbreviation	Up- or down-regulation	Ratio1	Ratio2
Cell cycle					*Oxidative phosphorylation*				
CR616879	CCNA1	↑	3.0672	3.0644	AF020351	*NDUFS4	↓	0.3385	0.4096
U03106	CDKN1A	↓	0.2809	0.2452					
CAG46598	PCNA	↑	2.7062	2.4293	*Transport*				
					U49248	*ABCC2	↑	2.4615	3.0030
Apoptosis					X78338	*ABCC1	↑	2.3313	3.4222
BC008678	IL1B	↓	0.4557	0.4570					
NM_001191	BCL2L1	↑	2.8732	3.0117	*Interaction*				
					X03168	*VTN	↑	2.3919	2.0326
Signaling pathway					BC066552	*LAMA4	↑	2.7738	2.0726
BC023523	*DGKA	↓	0.4739	0.4493	NM_002985	*CCL5	↑	2.3735	2.5161
BC026331	*ITPKA	↓	0.4398	0.5029	J03171	*IFNAR1	↑	2.7647	2.2603
Y11312	#PIK3C2B	↑	2.3524	2.2097	L08096	*TNFSF7	↓	0.3164	0.3183
U15932	*DUSP5	↓	0.4698	0.5024	X04430	IL6	↑	2.0441	2.0289
BX640908	*EVI1	↑	2.2908	3.6488	L04270	*LTBR	↓	0.5413	0.4026
BC036092	*MAX	↑	2.0580	2.1085	BC047698	*IL7	↑	2.6382	3.6129
L11285	#MAP2K2	↑	2.4983	2.7410	U31628	*IL15RA	↑	2.1865	1.9884
BC037236	*DUSP6	↓	0.3693	0.4193	BC030155	*TNFRSF11B	↓	0.3813	0.4669
U67206	#CASP7	↓	0.4484	0.4970	CR602522	*EDN1	↑	3.8264	3.6028
AY054395	*BDNF	↑	2.4910	2.1162	BC035618	*SSTR1	↑	2.7734	2.7338
M68874	#PLA2G4A	↑	2.4025	2.5646	BC034393	*EDN2	↑	3.2057	1.6309
X52479	#PRKCA	↑	5.2584	5.5842					
Y10256	#MAP3K14	↑	2.2107	2.1948	*Cell adhesion*				
CR612719	*GADD45A	↓	0.3957	0.1692	AB000712	*CLDN4	↑	3.0259	3.0188
CR618407	BMP2	↓	0.3782	0.4479	AB037787	*NLGN2	↓	0.4008	0.4931
M34057	*LTBP1	↑	2.0486	2.3859	AK075334	*MPZL1	↑	2.0453	2.3812
S78825	ID1	↓	0.4211	0.5100	AJ011497	*CLDN7	↓	0.2295	0.2684
M31682	*INHBB	↑	2.3259	2.0402	AF125377	*SNAI1	↓	0.4816	0.4511
AF048722	*PITX2	↓	0.4366	0.4842	X02761	*FN1	↓	0.0503	0.0659
L38969	*THBS3	↑	2.6254	2.3153	AK001655	*PARVA	↑	2.5954	1.9570
BC027958	*BMP5	↑	27.3978	14.6852	AF070648	*CAV1	↓	0.2474	0.3467
CR749295	*BTRC	↓	0.4133	0.5503	BC005256	*CAV2	↓	0.4596	0.2935
AY009401	#WNT6	↑	2.2685	2.2062	BX641139	*SHC3	↓	0.4779	0.4600
AF016507	*CTBP2	↑	2.5090	2.4220					
AB027464	#FZD10	↑	2.1476	2.2260	*Cell Communication*				
AL110263	*PDE1A	↓	0.0585	0.0036	AK056254	*KRT4	↑	4.8146	3.3134
CR541865	*TNNC1	↑	4.7137	3.2209					
AK090868	*GNAL	↑	4.6538	2.9530	*Regulation of actin cytoskeleton*				
J04164	*IFITM1	↓	0.2604	0.3697	BC000114	*MATK	↓	0.3410	0.4210
AK000507	*DDIT4	↓	0.2913	0.3634	BC036756	*GNA13	↓	0.4721	0.4635
U36798	*PDE3A	↑	2.9651	2.4967	BF965156	RRAS	↓	0.4435	0.4023
					M59911	*ITGA3	↓	0.4539	0.4284
Leukocyte transendothelial migration					AK125819	*GSN	↓	0.3614	0.2474
AL832088	MMP2	↓	0.1769	0.1513	X06256	ITGA5	↓	0.3154	0.3152
					D45906	*LIMK2	↓	0.3485	0.2934
Natural killer cell mediated cytotoxicity					X53587	*ITGB4	↓	0.3316	0.3682
Q99706	*KIR2DL4	↑	3.1394	2.6300	AK026977	*MYH10	↑	2.2017	2.4169
BC034689	*ULBP2	↓	0.4308	0.4985	AL096719	*PFN2	↑	2.2427	2.7714
BC035416	*ULBP1	↑	2.3254	2.3926	X17033	*ITGA2	↓	0.2675	0.2783

Accession No	Abbreviation	Up- or down-regulation	Ratio1	Ratio2
Metabolism				
AK127770	*PDE9A	↓	0.3546	0.5053
X02994	*ADA	↓	0.4653	0.4197
D12485	*ENPP1	↑	2.5975	1.6024
U67733	*PDE2A	↑	5.2929	3.2765
BG682813	*POLE4	↑	2.6344	1.7177
X55740	*NT5E	↑	1.9939	2.5385
AK123345	*PKM2	↑	2.0849	2.2023
AK074134	*SLC27A3	↓	0.3055	0.3450
D13643	*DHCR24	↑	1.7296	2.5274
D88308	*SLC27A2	↑	2.7027	2.1881
U34683	*GSS	↓	0.4683	0.4188
X03674	*G6PD	↑	2.1507	2.5817
L35546	*GCLM	↑	2.3915	3.9486
CR614504	*GSTM3	↑	2.3722	2.5401
BC020744	*AKR1C4	↑	4.6412	4.8338
S70154	*ACAT2	↓	0.0156	0.0041
BC004102	*ALDH3A1	↑	5.0622	5.3780
AF030555	*ACSL4	↓	0.4089	0.5404
D13900	*ECHS1	↓	0.4890	0.4808
CR601714	*ME1	↑	1.9955	2.1160
AB031478	*ACP6	↑	2.5841	2.1902
AK025732	*ASAH1	↑	2.1362	2.0824
BC070060	*SGPP1	↑	2.6498	1.7846
AK095578	*SPHK1	↓	0.2473	0.2105
M15856	*LPL	↑	8.8089	12.5624
M57892	*CA6	↑	2.1346	3.0340
D90282	*CPS1	↑	2.2087	2.8370
M12267	*OAT	↓	0.0393	0.1207
BC011831	*MMAB	↑	2.4665	1.6824
D63391	*PAFAH1B3	↓	0.5393	0.4115
BC001482	*PISD	↓	0.4591	0.5443
AF523360	*HNMT	↑	3.3276	2.2063
M61831	*AHCY	↓	0.4089	0.3775
U89942	LOXL2	↑	1.9654	2.1514
AK131096	*GALNS	↓	0.4241	0.5482
U03056	*HYAL1	↓	0.2634	0.5182
BC014139	*ALPPL2	↓	0.2423	0.5194
BC009647	*ALPP	↑	2.0290	2.3588
M62783	*NAGA	↓	0.2378	0.3437
U12778	*ACADSB	↓	0.4079	0.4722
BC017338	*FUCA1	↓	0.4378	0.3032
AB016247	*SC5DL	↑	3.3849	3.2823
AB015630	*B3GNT3	↓	0.2042	0.2731
AK095746	*B3GNT4	↓	0.5518	0.4466
BC017249	*ENO3	↑	1.9912	2.6999
D14697	*FDPS	↓	0.4835	0.4999
AK096313	*CARS	↑	2.0912	2.1213
X91257	*SARS	↑	2.1797	2.4608

Accession No	Abbreviation	Up- or down-regulation	Ratio1	Ratio2
AK074524	*GARS	↑	1.9285	2.2692
AK129934	PCK2	↑	1.7061	2.7548
NM_000963	PTGS2	↑	3.4100	3.4133
Hematopoietic cell lineage				
AK125531	*CD24	↑	2.9598	2.3196
M22324	*ANPEP	↓	0.2580	0.1899
J03779	*MME	↓	0.3872	0.4473
AK074082	*EPOR	↑	2.3909	2.4391
Complement and coagulation cascades				
M14113	*F8	↑	1.9940	2.5842
M57729	*C5	↑	3.3546	2.6310
BX649164	*SERPINE1	↓	0.1994	0.1417
BC013575	PLAU	↓	0.3667	0.4330
CR601067	PLAUR	↓	0.2728	0.2455
J02931	*F3	↑	2.5378	2.5057
M14338	*PROS1	↓	0.5346	0.4295
BC005378	*C4BPB	↑	5.0472	4.1054
Carbon fixation				
L12711	*TKT	↑	2.0682	2.2488
Tight junction				
Z15108	#PRKCZ	↓	0.4353	0.4319
AK025615	*BCAT1	↑	4.2197	2.0964
Long-term depression				
D26070	*ITPR1	↑	3.6304	3.7319
Axon guidance				
M57730	*EFNA1	↑	2.4792	2.9131
AF040990	*ROBO1	↑	4.4963	2.7992
CR749333	*NRP1	↓	0.4256	0.5860
Ribosome				
X69150	*RPS18	↓	0.4647	0.3602
Huntington's disease				
M55153	*TGM2	↓	0.3356	0.2605
Alzheimer's disease				
AF178532	*BACE2	↓	0.3260	0.2350
Neurodegenerative disorders				
AB020652	*NEFH	↓	0.1642	0.0152

Note: Genes marked * have not been reported to associate with HBx in literature. Genes marked # have been reported to indirectly associate with HBx in literature.

used was the fluorescence-exchange microarray. Additionally, we performed three independent cDNA microarray

analyses to get more precise data. In Table 1, the expression of the selected candidates was either up- or down-regulated

by at least two folds. When compared with the differential expression profiles in H7402-X cells[10], we found that the data from the differential expression profiles in L-O2-X cells differed substantially. Only three genes, PCNA, BMP2, and IL-6, were altered in both H7402-X cells and L-O2-X cells.

HBx was responsible for the upregulation of PCNA and Bcl-2 To further validate the candidate genes in the cDNA microarray and to preliminarily investigate the molecular alterations of proliferating cell nuclear antigen (PCNA) and Bcl-2 in the L-O2-X cell line, we examined the regulation of PCNA and Bcl-2 at the protein level by Western blot analysis. The data showed that the expression levels of PCNA and Bcl-2 were increased in L-O2-X cells (Figure 2A). We further confirmed the findings by applying Glyco Band-Scan software (PROZYME, San Leandro, CA, USA; Figure 2C). Moreover, we investigated the effect of HBx on the regulation of PCNA and Bcl-2 by RNA interference (RNAi)

targeting HBx mRNA. After transfection, the RNAi resulted in the decrease of PCNA and Bcl-2 within 48 h (Figure 2B), suggesting that HBx was responsible for the upregulation of PCNA and Bcl-2. These data were further confirmed by Glyco BandScan software (PROZYME, San Leandro, CA, USA; Figure 2D).

The upregulation of COX-2, mediated by HBx, contributed to the proliferation As shown in Table 1, the COX-2 gene was upregulated in L-O2-X cells. We provided evidence by Western blot analysis that the expression of COX-2 at the protein level was higher in L-O2-X cells than in L-O2 cells (Figure 3A). The downregulation of HBx mediated by RNAi in L-O2-X cells abolished the upregulation of COX-2 (Figure 3A). We further confirmed the findings by applying Glyco BandScan software (PROZYME, San Leandro, CA, USA; Figure 3B). Next, we demonstrated the effect of COX-2 on proliferation using the BrdU incorporation assay. The data showed that the percentage of cells in the S phase significantly increased in L-O2-X cells (*P*<0.05, *vs* L-O2 cells, Student's *t* test). However, enhanced proliferation in L-O2-X cells was abolished by treatment with indomethacin (indo, an inhibitor of COX-2, Sigma-Aldrich,
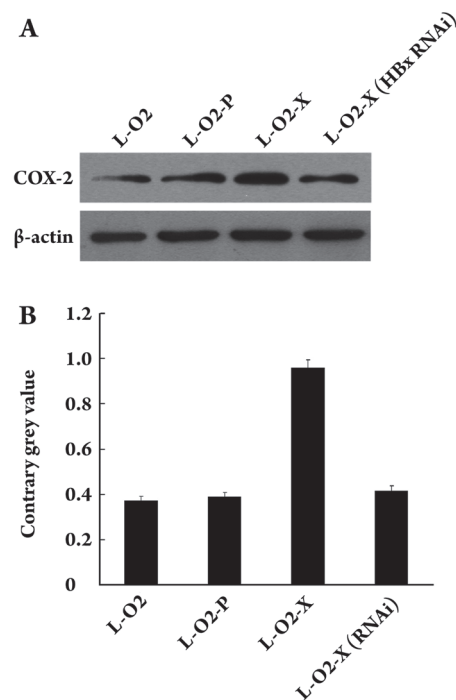

Figure 2. HBx upregulated the expression of PCNA and Bcl-2. (A) Western blot analysis showed that the expression levels of PCNA and Bcl-2 were upregulated in L-O2-X cells. HBx was detectable in L-O2-X cells. (B) PCNA, Bcl-2 and HBx protein were downregulated by transfection with pSilencer 3.0-X plasmid encoding silencing RNA, which targets HBx mRNA in L-O2-X cells. (C, D) The histogram shows the results from applying Glyco Band-Scan software.

Figure 3. HBx was responsible for the upregulation of COX-2, as indicated by Western blotting. (A) COX-2 was upregulated in L-O2-X cells. Transfection with the pSilencer 3.0-X plasmid encoding silencing RNA, which targets HBx mRNA, could abolish the tendency. (B) The histogram shows the results of applying Glyco Band-Scan software.

USA) (Figure 4), suggesting that HBx was able to upregulate COX-2, which contributed to the proliferation. No statistically significant difference was observed between L-O2 cells and cells transfected with empty pcDNA3 vector (termed L-O2-P).
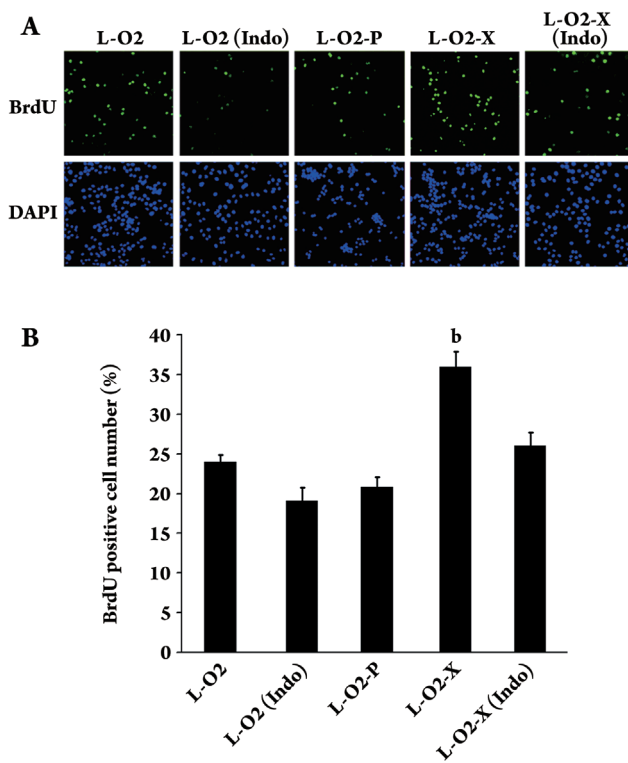
Discussion

Figure 4. The upregulation of COX-2, mediated by HBx, contributed to proliferation and is shown by BrdU incorporation assay. Positive DAPI (4,6-diamidino-2-phenylindole dihydrochloride hydrate, Sigma) staining was shown by blue fluorescence in the nuclei of cells. Green fluorescence showed the number of BrdU positive cells. (A) The BrdU incorporation assay showed that proliferation was higher in the L-O2-X cells relative to L-O2 cells ([b]$P < 0.05$, L-O2-X *vs* L-O2 cells, Student's *t* test). (B) The histogram represents three independent experiments with standard errors, shown as error bars.

HBx plays a crucial role in HBV-related pathogenesis. Some research groups have investigated the gene expression profiles associated with HBx. However, our data differ markedly from that data in these reports[17, 18]. HBx can lead to contradictory findings, largely because of the use of different cell types and transformed cells. In the present study, we chose an immortalized human liver cell line as a model to show the basic response of host cells to the HBx gene.

Using a cDNA microarray technique, we identified and classified the genes that were altered as a result of their involvement in an HBx-mediated process (Figure 1). Our findings showed that 82 genes were upregulated and 70 genes were downregulated in L-O2-X cells (Table 1). Most were involved in the cell cycle, signal pathways, metastasis, immune response, metabolism, and other processes. Table 1 shows that many genes that have not been reported to associate with HBx in the literature were found by microarray assay, which provides us with valuable clues for the further investigation of HBx. Our data showed that cyclin A1, PCNA and Bcl-2 were upregulated, whereas p21 was simultaneously downregulated. Furthermore, the altered expression of PCNA and Bcl-2 was verified by Western blot analysis (Figure 2). HBx upregulates PCNA by increasing the recruitment of CBP/p300 to endogenous PCNA promoters[19]. Our microarray data were consistent with this report. Cyclin A1, a member of the cyclin A family, is related to some types of carcinogenesis[20]. p21 is a negative regulator of the cell cycle. BCL-2 family members form hetero- or homodimers and act as anti- or pro-apoptotic regulators that are involved in a wide variety of cellular activities. Cyclin-dependent kinases (CDKs) and cyclin-dependent kinase inhibitors (CKIs) play important roles in controlling cell proliferation, differentiation, and apoptosis. Defects in cell cycle regulation are common causes of the abnormal proliferation of cancer cells. Those proteins, which are mentioned above and are involved in the cell cycle and apoptosis, may greatly influence tumorigenesis. Another study indicates that many MAPK family members are upregulated in HBV-related HCC[10, 21]. Our present data showed that MAP2K2, MAP3K14 and MAX were upregulated, whereas Gadd45a was downregulated in L-O2-X cells; these changes may be related to rapid proliferation. All biological activities of c-Myc require its binding partner, Max[22]. c-Myc has been assigned roles in hepatocyte proliferation during liver development and regeneration, control of hepatic metabolism, and the dysregulated growth that occurs during heptocarcinogenesis[23–26]. Therefore, the enhancement of Max may be consistent with the induction of c-Myc in L-O2-X cells to promote hepatocyte growth and proliferation. In our experiments, Gadd45a, a p53-regulated and DNA damage inducible protein, was downregulated. Gadd45 plays a role in G2-M arrest in response to DNA damage. Gadd45 can bind to multiple important cellular proteins such as PCNA, p21 protein, MTK/MEKK4 — an upstream activator of the JNK pathway — and Cdc2 protein kinase. Furthermore, some reports show that Gadd45 can inhibit cell transformation and tumor progression[27, 28]. Signaling by the Wnt family of

secreted glycoproteins is essential both in normal embryonic cell-to-cell interactions and in the pathogenesis of a variety of diseases, including cancer[29]. First, Wnt proteins bind to receptors of the Frizzled and LRP families on the cell surface. Then, through several cytoplasmic relay components, the signal is transduced to activate transcription of Wnt target genes. Here, we found that both FZD10 (one of the Frizzled and LRP families) and CTBP2, which are involved in Wnt signaling, were increased. Additionally, BTRC, which may be a candidate for tumor-suppressive activities[30], was decreased in L-O2-X cells. Indeed, RNA interference-mediated knock-down of CtBP2 (C-terminal binding protein family proteins) decreases cell invasion, and ectopic expression of CtBP2 enhances tumor cell migration and invasion. Importantly, the overexpression of FZD10 (a cell-surface receptor for molecules in the Wnt pathway) acts as a potential contributor to synovial sarcomas. Moreover, a humanized antibody against FZD10 might be a promising treatment for patients with tumors that overexpress FZD10[31]. Secreted-type glycoprotein WNTs can bind to FZD10 to transduce signals to the β-catenin-TCF pathway, the JNK pathway, or the calcium signaling pathway. Accordingly, variation in the Wnt pathway and other signals affected by the Wnt pathway that were seen in our study may contribute to the early carcinogenesis mediated by HBx.

Interactions between cells and their surrounding extracellular matrix are essential for the proper execution and regulation of survival, proliferation, cytoskeletal organization, and migration. Furthermore, cell-extracellular matrix contact regulates physiological and pathological processes, such as development, differentiation, and metastasis. Laminins, a family of extracellular matrix glycoproteins, are the major noncollagenous constituents of the basement membrane. Some reports suggest that a strong correlation between the high expression of LAMA4 (one of laminin family) and tumor invasion and metastasis indicates that it is a novel marker for the processes of tumor invasion and metastasis[32]. Our microarray data showed that LAMA4 was upregulated in L-O2-X cells. The chemokine RANTES (regulated on activation normal T-cell expressed and secreted; CCL5) is a member of the CC-chemokine family, a group of small proteins with a highly conserved structure[33]. Using the cDNA microarray technique, we found that CCL5 was highly expressed in L-O2-X cells. Other studies indicate that CCL5s are inflammatory mediators with pro-malignancy activities in breast cancer and that they are shown to mediate many types of tumor-promoting cross-talk between the tumor cells and cells of the tumor microenvironment. Tumor-derived CCL5 can inhibit the T cell response and

enhance the growth of murine mammary carcinoma *in vivo*[34]. Interleukin-6 (IL-6) induces either differentiation or growth of a variety of cells and also plays a role in cell interaction. In our study, IL-6 was upregulated in L-O2-X cells relative to L-O2 cells. Binding of IL-6 to its receptor initiates cellular events including activation of JAK kinases and activation of ras-mediated signaling. In addition, it has been suggested that IL-6 participates in the malignant progression of prostate cancer[35]. Adhesion of tumor cells to host cell layers and subsequent migration are pivotal steps in cancer invasion and metastasis. Organization of the cytoskeleton and cell adhesion molecules plays an important role in this event. Some candidates in our study were related to these cell processes, including CLDN4, CLDN7, CAV1, and CAV2. The family of more than 20 claudin (CLDN) proteins comprises one of the major structural elements within the apical tight junction apparatus, a dynamic cellular nexus for maintenance of a luminal barrier, paracellular transport, and signal transduction. Loss of normal tight junction functions constitutes a hallmark of human carcinomas. CLDN4 proteins are maintained or elevated in breast, ovarian, pancreatic, and prostate cancers, whereas CLDN7 proteins are diminished in head, neck, and breast tumors[36]. The down-regulation of caveolin-1 (encoded by CAV1) and caveolin-2 (encoded by CAV2) is found in various types of primary tumors and cancer cell lines, indicating that these are candidate tumor suppressor genes[37, 38].

In our data, we also found that HBx greatly affected cellular metabolism, in which HBx upregulated the PTGS2 gene that encodes cyclooxygenase-2 (COX-2) (Figure 3). COX-2 is overexpressed in various cancers, including esophageal, gastric, colon, and pancreatic cancers[39]. It is possible that both tumor- and stroma-derived COX-2 could influence tumor proliferation, angiogenesis and/or immune function. Using the BrdU incorporation assay, we observed that HBx enhanced the proliferation of L-O2 cells by upregulating COX-2 (Figure 4). Our findings are concurrent with a report that HBx induces COX-2 through the activation of NF-AT to promote tumor cell invasion and metastasis[40]. LOXL2 catalyzes the crosslinking of collagen and elastin in the extracellular matrix and is assumed to be involved in tumor progress and cell adhesion. Some findings support the presumption that LOXL2 plays a role in malignant transformation[41, 42].

In this study, we found that only three genes, PCNA, BMP2 and IL-6, were altered in both H7402-X cells and L-O2-X cells. We considered the possibility that HBx may affect gene expression in different ways in hepatoma H7402 cells and L-O2 liver cells because the genetic background is different. The gene expression profiles mediated by HBx in

L-O2 cells may reflect alterations in the early stage of carcinogenesis.

Our study has revealed some novel candidate genes by cDNA microarray analysis (Table 2) that provide new insight into the pathogenesis mediated by HBx. Consequently, an understanding of the molecular mechanisms involved in this dynamic process will aid in identifying novel potential targets for earlier diagnosis and more specific therapies.

Table 2. Genes significantly altered in L-02-X cells and their classifications in signal pathway.

Accession No	Abbreviation	Up- or down-regulation	Name
Cell cycle			
CR616879	CCNA1	↑	cyclin A1
U03106	CDKN1A	↓	cyclin-dependent kinase inhibitor 1A (p21, Cip1)
CAG46598	PCNA	↑	proliferating cell nuclear antigen
Apoptosis			
NM_001191	BCL2L1	↑	Bcl2 interacting mediator 1 of cell death
Signaling pathway			
MAPK signaling pathway			
BC036092	MAX	↑	MAX protein
L11285	MAP2K2	↑	mitogen-activated protein kinase kinase 2
M68874	PLA2G4A	↑	Cytosolic phospholipase A2 (cPLA2)
X52479	PRKCA	↑	PKC-alpha
Y10256	MAP3K14	↑	Mitogen-activated protein kinase kinase kinase 14
CR612719	GADD45A	↓	Growth arrest and DNA-damage-inducible protein GADD45 alpha
Wnt signaling pathway			
CR749295	BTRC	↓	beta-transducin repeat containing
AY009401	WNT6	↑	wingless-type MMTV integration site family, member 6
AF016507	CTBP2	↑	C-terminal binding protein 2
AB027464	FZD10	↑	frizzled homolog 10
Interaction			
BC066552	LAMA4	↑	laminin, alpha 4
NM_002985	CCL5	↑	chemokine (C-C motif) ligand 5
X04430	IL6	↑	interleukin 6
Cell adhesion			
AB000712	CLDN4	↑	claudin 4
AJ011497	CLDN7	↓	claudin 7
AF070648	CAV1	↓	Caveolin-1
BC005256	CAV2	↓	Caveolin-2
Arachidonic acid metabolism			
U89942	LOXL2	↑	Lysyl oxidase related protein 2
NM_000963	PTGS2	↑	Cyclooxygenase -2

Author contribution

Prof Xiao-dong ZHANG and Li-hong YE designed the research; Wei-ying ZHANG performed the research; Prof Rong XIANG discussed the research; Fu-qing XU and Chang-liang SHAN help to perform part of the research. Wei-ying ZHANG analyzed the data and wrote the paper. Prof Xiao-dong ZHANG revised the paper.

References

1   Zhang XD, Zhang WY, Ye LH. Pathogenesis of hepatitis B virus infection. Future Virol 2006; 1: 637–47.

2   Feitelson MA, Sun B, Satiroglu Tufan NL, Liu J, Pan J, Lian Z. Genetic mechanisms of hepatocarcinogenesis. Oncogene 2002; 21: 2593–604.

3   Okuda K. Hepatocellular carcinoma. J Hepatol 2000; 32: 225–37.

4   Zhang XD, Zhang H, Ye LH. Effects of hepatitis B virus X protein on the development of liver cancer. J Lab Clin Med 2006; 147: 58–66.

5   Henkler FF, Koshy R. Hepatitis B virus transcriptional activators: mechanisms and possible role in oncogenesis. J Viral Hepat 1996; 3: 109–21.

6   Su JM, Lai XM, Lan KH, Li CP, Chao Y, Yen SH, *et al*. X protein of hepatitis B virus functions as a transcriptional corepressor on the human telomerase promoter. Hepatology 2007; 46: 402–13.

7   Yun C, Cho H, Kim SJ, Lee JH, Park SY, Chan GK, *et al*. Mitotic aberration coupled with centrosome amplification is induced by hepatitis B virus X oncoprotein via the Ras-mitogen-activated protein/extracellular signal-regulated kinase-mitogen- activated protein pathway. Mol Cancer Res 2004; 2: 159–69.

8   Zhang XD, Dong N, Zhang H, You JC, Wang HH, Ye LH. Effects of hepatitis B virus X protein on human telomerase reverse transcriptase expression and activity in hepatoma cells. J Lab Clin Med 2005; 145: 98–104.

9   Zhang XD, Dong N, Yin LH, Cai N, Ma HT, You JC, *et al*. Hepatitis B virus X protein upregulates survivin expression in hepatoma tissues. J Med Virol 2005; 77: 374–81.

10 Ye LH, Dong N, Wang Q, Xu ZL, Cai N, Wang HH, *et al*. Progressive changes in hepatoma cells stably transfected with hepatitis B virus X gene. Intervirology 2008; 51: 50–8.

11 Huang R, Xing Z, Luan Z, Wu T, Wu X, Hu G. A specific splicing variant of SVH, a novel human armadillo repeat protein, is up-regulated in hepatocellular carcinomas. Cancer Res 2003; 63: 3775–82.

12 Huang R, Wu T, Xu L, Liu A, Ji Y, Hu G. Upstream binding factor up-regulated in hepatocellular carcinoma is related to the survival and cisplatin-sensitivity of cancer cells. FASEB J 2002; 16: 293–301.

13 Zhang H, Shan CL, Li N, Zhang X, Zhang XZ, Xu FQ, *et al*. Identification of a natural mutant of HBV X protein truncated 27 amino acids at the COOH terminal and its effect on liver cell proliferation. Acta Pharmacol Sin 2008; 29: 473–80.

14 Wang YD, Chen WD, Wang M, Yu D, Forman BM, Huang W. Farnesoid X receptor antagonizes nuclear factor kappaB in hepatic inflammatory response. Hepatology 2008; 48: 1632–43.

15 Wang FZ, Sha L, Ye LH, Zhang XD. Promotion of cell proliferation by HBXIP via upregulation of human telomerase reverse transcriptase in human mesenchymal stem cells. Acta Pharmacol Sin 2008; 29: 83–9.

16 Lengronne A, Pasero P, Bensimon A, Schwob E. Monitoring S phase progression globally and locally using BrdU incorporation in TK (+) yeast strains. Nucleic Acids Res 2001; 29: 1433–42.

17 Ng RK, Lau CY, Lee SM, Tsui SK, Fung KP, Waye MM. cDNA microarray analysis of early gene expression profiles associated with hepatitis B virus X protein-mediated hepatocarcinogenesis. Biochem Biophys Res Commun 2004; 322: 827–35.

18 Hu Z, Zhang Z, Kim JW, Huang Y, Liang TJ. Altered proteolysis and global gene expression in hepatitis B virus X transgenic mouse liver. J Virol 2006; 80: 1405–13.

19 Lara-Pezzi E, Gómez-Gaviro MV, Gálvez BG, Mira E, Iñiguez MA, Fresno M, *et al*. The hepatitis B virus X protein promotes tumor cell invasion by inducing membrane-type matrix metallo-proteinase-1 and cyclooxygenase-2 expression. J Clin Invest 2002; 110: 1831–8.

20 Cheng KY, Noble ME, Skamnaki V, Brown NR, Lowe ED, Kontogiannis L, *et al*. The role of the phospho-CDK2/cyclinA recruitment site in substrate recognition. J Biol Chem 2006; 281: 23167–79.

21 Xu XR, Huang J, Xu ZG, Qian BZ, Zhu ZD, Yan Q, *et al*. Insight into hepatocellular carcinogenesis at transcriptome level by comparing gene expression profiles of hepatocellular carcinoma with those of corresponding noncancerous liver. Proc Natl Acad Sci USA 2001; 98: 15089–94.

22 Blackwood EM, Luscher B, Eisenman RN. Myc and max associate *in vivo*. Genes Dev 1992; 6: 71–80.

23 Collier JJ, Doan TT, Daniels MC, Shurr JR, Kolls JK, Scott DK. c-Myc is required for the glucose-mediated induction of metabolic enzyme genes. J Biol Chem 2003; 278: 6588–95.

24 Kim S, Li Q, Dang CV, Lee LA. Induction of ribosomal genes and hepatocyte hypertrophy by adenovirus-mediated expression of c-Myc *in vivo*. Proc Natl Acad Sci USA 2000; 97: 11198–202

25 Riu E, Ferre T, Mas A, Hildago A, Franckhauser S, Bosch F. Overexpression of c-myc in diabetic mice restores altered expression of the transcription factor genes that regulate liver metabolism. Biochem J 2002; 368: 931–7.

26 Thompson NL, Mead JE, Braun L, Goyette M, Shank PR, Fausto N. Sequential protooncogene expression during rat liver regeneration. Cancer Res 1986; 46: 3111–7.

27 Ji JF, Wu Y, Zhan Q. Gadd45a function in suppressing cell transformation and tumor malignancy. Prog Biochem Biophys 2006; 12: 1146–53.

28 Zhan Q, Lord KA, Alamo IJ, Hollander MC, Carrier F, Ron D, *et al*. The gadd and MyD genes define a novel set of mammalian genes encoding acidic proteins that synergistically suppress cell growth. Mol Cell Biol 1994; 14: 2361–71.

29 Nusse R. Wnt signaling in disease and in development. Cell Res 2005; 15: 28–32.

30 Fujiwara T, Suzuki M, Tanigami A, Ikenoue T, Omata M, Chiba T, *et al*. The BTRC gene, encoding a human F-box/WD40-repeat protein, maps to chromosome 10q24-q25. Genomics 1999; 58: 104–5.

31 Nagayama S, Fukukawa C, Katagiri T, Okamoto T, Aoyama T, Oyaizu N, *et al*. Therapeutic potential of antibodies against

FZD10, a cell-surface protein, for synovial sarcomas. Oncogene 2005; 24: 6201–12.

32 Huang X, Ji G, Wu Y, Wan B, Yu L. LAMA4, highly expressed in human hepatocellular carcinoma from Chinese patients, is a novel marker of tumor invasion and metastasis. J Cancer Res Clin Oncol 2008; 134: 705–14.

33 Zlotnik A, Yoshie O. Chemokines: a new classification system and their role in immunity. Immunity 2000; 12: 121–7.

34 Tyner JW, Uchida O, Kajiwara N, Kim EY, Patel AC, O'Sullivan MP, *et al*. CCL5-CCR5 interaction provides antiapoptotic signals for macrophage survival during viral infection. Nat Med 2005; 11: 1180–7.

35 Smith, PC, Hobish A, Lin, D L, Culig Z, Keller ET. Interleukin-6 and prostate cancer progression. Cytokine Growth Factor Rev 2001; 12: 33–40.

36 Kominsky SL, Argani P, Korz D, Evron E, Raman V, Garrett E, *et al*. Loss of the tight junction protein claudin-7 correlates with histological grade in both ductal carcinoma *in situ* and invasive ductal carcinoma of the breast. Oncogene 2003; 22: 2021–33.

37 Wiechen K, Diatchenko L, Agoulnik A, Scharff KM, Schober H, Arlt K, *et al*. Caveolin-1 is down-regulated in human ovarian carcinoma and acts as a candidate tumor suppressor gene. Am J Pathol 2001; 159: 1635–43.

38 Fiucci G, Ravid D, Reich R, Liscovitch M. Caveolin-1 inhibits anchorage independent growth, anoikis and invasiveness in MCF-7 human breast cancer cells. Oncogene 2002; 21: 2365–75.

39 Koga T, Shibahara K, Kabashima A, Sumiyoshi Y, Kimura Y, Takahashi I, *et al*. Altered proteolysis and global gene expression in hepatitis B virus X transgenic mouse liver. Hepatogastroenterology 2004; 51: 1626–30.

40 Cougot D, Wu Y, Cairo S, Caramel J, Renard CA, Lévy L, *et al*. The hepatitis B virus X protein functionally interacts with CREB-binding protein/p300 in the regulation of CREB-mediated transcription. J Biol Chem 2007; 282: 4277–87.

41 Rost T, Pyritz V, Rathcke IO, Görögh T, Dünne AA, Werner JA. Reduction of LOX- and LOXL2-mRNA expression in head and neck squamous cell carcinomas. Anticancer Res 2003; 23: 1565–73.

42 Schmidt H, Semjonow A, Csiszar K, Korsching E, Brandt B, Eltze E. Mapping of a deletion interval on 8p21-22 in prostate cancer by gene dosage PCR. Verh Dtsch Ges Pathol 2007; 91: 302–7.